MCB
Journals.ASM.org

The C2 Domain and Altered ATP-Binding Loop Phosphorylation at Ser^{359} Mediate the Redox-Dependent Increase in Protein Kinase C-δ Activity

Jianli Gong,[a] Yongneng Yao,[a] Pingbo Zhang,[b] Barath Udayasuryan,[d] Elena V. Komissarova,[a] Ju Chen,[c] Sivaraj Sivaramakrishnan,[d] Jennifer E. Van Eyk,[b] Susan F. Steinberg[a]

Department of Pharmacology, Columbia University, New York, New York, USA[a]; Department of Medicine, Johns Hopkins School of Medicine, Baltimore, Maryland, USA[b]; University of California, San Diego, School of Medicine, La Jolla, California, USA[c]; Department of Cell and Developmental Biology and Department of Biomedical Engineering, University of Michigan, Ann Arbor, Michigan, USA[d]

The diverse roles of protein kinase C-δ (PKCδ) in cellular growth, survival, and injury have been attributed to stimulus-specific differences in PKCδ signaling responses. PKCδ exerts membrane-delimited actions in cells activated by agonists that stimulate phosphoinositide hydrolysis. PKCδ is released from membranes as a Tyr^{313}-phosphorylated enzyme that displays a high level of lipid-independent activity and altered substrate specificity during oxidative stress. This study identifies an interaction between PKCδ's Tyr^{313}-phosphorylated hinge region and its phosphotyrosine-binding C2 domain that controls PKCδ's enzymology indirectly by decreasing phosphorylation in the kinase domain ATP-positioning loop at Ser^{359}. We show that wild-type (WT) PKCδ displays a strong preference for substrates with serine as the phosphoacceptor residue at the active site when it harbors phosphomimetic or bulky substitutions at Ser^{359}. In contrast, PKCδ-S359A displays lipid-independent activity toward substrates with either a serine or threonine as the phosphoacceptor residue. Additional studies in cardiomyocytes show that oxidative stress decreases Ser^{359} phosphorylation on native PKCδ and that PKCδ-S359A overexpression increases basal levels of phosphorylation on substrates with both phosphoacceptor site serine and threonine residues. Collectively, these studies identify a C2 domain-pTyr^{313} docking interaction that controls ATP-positioning loop phosphorylation as a novel, dynamically regulated, and physiologically relevant structural determinant of PKCδ catalytic activity.

Protein kinase C-δ (PKCδ) is a serine/threonine kinase that plays a key role in signal transduction pathways that control a wide range of cellular responses. PKCδ contains a highly conserved C-terminal catalytic domain and N-terminal regulatory C1 and C2 domains. The C1 domain binds lipids and anchors full-length PKCδ to membranes. The functional role of the C2 domain has remained more elusive. While C2 domains of conventional PKC (cPKC) isoforms function as calcium-regulated membrane-targeting modules, the PKCδ C2 domain is a topological variant that does not coordinate calcium or bind lipids (1). Rather, it has been characterized as a protein-protein interaction motif (2, 3), with recent evidence that the PKCδ-C2 domain is a phosphotyrosine (pY) binding motif that binds the consensus sequence (Y/F)-(S/A)-(V/I)-pY-(Q/R)-X-(Y/F) (4).

PKCδ is allosterically activated by lipids (diacylglycerol [DAG] or phorbol esters such as phorbol 12-myristate 13-acetate [PMA]) that bind to the C1 domain. PKCδ also is dynamically regulated as a result of tyrosine phosphorylation by Src (5, 6). We previously showed that oxidative stress releases PKCδ from membranes, activates Src, and induces a global increase in PKCδ phosphorylation at Tyr^{313} and Tyr^{334} in both soluble and particulate subcellular compartments (7). These residues in the V3 hinge region of human PKCδ correspond to Tyr^{311} and Tyr^{332} in rodent PKCδ. The nomenclature for human PKCδ is used below. While PMA does not increase Src activity, it delivers PKCδ in an active conformation to Src-enriched caveolar membranes where a low level of basal Src activity is sufficient to promote PKCδ phosphorylation at Tyr^{313} but not Tyr^{334} (8). Since PKCδ is phosphorylated by Src *in vitro* at both Tyr^{313} and Tyr^{334} (9), a mechanism that might account for the selective PMA-dependent PKCδ phosphorylation at Tyr^{313} but not Tyr^{334} has never been obvious.

Stimulus-induced increases in PKCδ-Tyr^{313} phosphorylation have been implicated in several PKCδ-dependent cellular responses (10, 11). We previously showed that Tyr^{313} phosphorylation influences PKCδ activity toward cardiac troponin I (cTnI, the inhibitory subunit of the troponin complex and a physiologically important PKCδ substrate in cardiomyocytes) (9). cTnI contains several phosphorylation clusters that exert distinct effects on cardiac contraction. PKCδ phosphorylates cTnI at Ser^{23}/Ser^{24} when allosterically activated by phosphatidylserine (PS)/PMA; studies in detergent-extracted single cardiomyocytes link cTnI-Ser^{23}/Ser^{24} phosphorylation to a decrease in tension at submaximum, but not maximum, calcium concentrations. When PKCδ is tyrosine phosphorylated by Src, PKCδ acquires cTnI-Thr^{144} kinase activity: it phosphorylates cTnI at both Ser^{23}/Ser^{24} and Thr^{144},

Received 4 February 2015 **Accepted** 24 February 2015
Accepted manuscript posted online 9 March 2015
Citation Gong J, Yao Y, Zhang P, Udayasuryan B, Komissarova EV, Chen J, Sivaramakrishnan S, Van Eyk JE, Steinberg SF. 2015. The C2 domain and altered ATP-binding loop phosphorylation at Ser^{359} mediate the redox-dependent increase in protein kinase C-δ activity. Mol Cell Biol 35:1727–1740. doi:10.1128/MCB.01436-14.
Address correspondence to Susan F. Steinberg, sfs1@columbia.edu.
Supplemental material for this article may be found at http://dx.doi.org/10.1128/MCB.01436-14.

doi:10.1128/MCB.01436-14

leading to a decrease in maximum tension and cross-bridge kinetics (i.e., a different functional response). Additional studies showing that the Src-dependent acquisition of cTnI-Thr^{144} kinase activity is completely abrogated by a Y313F substitution implicates Tyr^{313} phosphorylation as the mechanisms underlying the Src-dependent increase in PKCδ activity (9).

The structural basis for Tyr^{313} phosphorylation-dependent changes in PKCδ's enzymology is not obvious. This study builds upon the intriguing observation that Tyr^{313} resides in a PKCδ-C2 domain consensus-binding motif (VGI-Y^{313}-QGF) (4) to show that the C2 domain interacts with the Tyr^{313}-phosphorylated V3 region and that this interaction controls PKCδ catalytic activity indirectly by regulating phosphorylation at Ser^{359}, a novel phosphorylation site in the Gly-rich ATP-positioning loop (G loop, also known as the phosphate binding P loop) of the kinase domain.

MATERIALS AND METHODS

Materials. PKCδ and PKCδ-pTyr^{334} antibodies were from Santa Cruz Biotechnology. Mouse monoclonal anti-green fluorescent protein (anti-GFP) 3E6 was from Invitrogen. Anti-Flag was from Sigma. All other antibodies were from Cell Signaling Technology. The specificity of all anti-PKCδ antibodies (including phosphorylation site-specific antibodies that specifically recognize phosphorylation at Thr^{507}, Tyr^{313}, and Tyr^{334}) has been validated previously (9). Src was from Invitrogen-Life Technologies. CREBtide and other peptide substrates were from Anaspec. PMA was from Sigma. Other chemicals were reagent grade.

Plasmids and cell lines. Mutant constructs of the PKCδ-enhanced GFP (EGFP) expression plasmid (human sequence with EGFP fused to its C terminus) (9) were generated by PCR and validated by sequencing. N-terminal Flag-tagged versions of PKCδ, PKCδ-ΔC2 (where ΔC2 represents a C2 deletion of amino acids [aa] 1 to 123 [Δ1-123]), and PKCδ-S359A also were generated and inserted into pcDNA3.1. All results shown in Fig. 2 and 3 with EGFP-tagged enzymes were replicated with Flag-tagged enzymes. Expression vectors were introduced into HEK293 cells (maintained in Dulbecco's modified Eagle's medium [DMEM] with 10% fetal bovine serum [FBS]) using Effectene transfection reagent (Qiagen) according to the manufacturer's instructions. Cells were lysed after 24 h in homogenization buffer containing 20 mM Tris-Cl (pH 7.5), 0.05 mM EDTA, 0.5 mM dithiothreitol (DTT), 0.2% Triton X-100, 5 μg/ml aprotinin, 5 μg/ml leupeptin, 5 μg/ml benzamidine, 1 mM phenylmethylsulfonyl fluoride, and 5 μM pepstatin A.

Cardiomyocytes were isolated from the hearts of 2-day-old Wistar rats and infected with adenoviral vectors that drive expression of wild-type PKC-δ (WT-PKCδ) or PKCδ-S359A according to methods published previously (12). Total cell lysates and fractions enriched in myofibrillar proteins were prepared according standard methods described in previous publications (7, 13). The study was approved by Columbia University's Institutional Animal Care and Use Committee.

Preparation of caveolar membranes. Caveolar membrane proteins were isolated according to a detergent-free purification scheme that was described previously (14).

IVKAs and Western blotting. *In Vitro* kinase assays (IVKAs) were performed with PKCδ immunoprecipitated with anti-GFP or anti-Flag from 150 μg of starting cell extract according to methods described previously (9). Incubations were performed for 30 min at 30°C in 110 μl of reaction buffer containing 30 mM Tris-Cl, pH 7.5, 5.45 mM $MgCl_2$, 0.65 mM EDTA, 0.65 mM EGTA, 0.1 mM DTT, 1.09 mM sodium orthovanadate, 0.1 μM calyculin, 0.55 μM protein kinase inhibitor (PKI), 217 mM NaCl, 3.6% glycerol, 89 μg/ml phosphatidylserine plus 175 nM PMA, and [γ-^{32}P]ATP (10 μCi, 66 μM) with 4 μg of Tn complex (consisting of equimolar cTnI, cTnT, and cTnC) as the substrate. Immunoblotting on lysates or immunoprecipitated PKCδ was according to methods described previously or to the manufacturer's instructions. In each figure, each panel represents the results from a single gel (exposed for a uniform duration); detection was with enhanced chemiluminescence. ^{32}P incorporation was quantified by phosphorimager, and PKCδ phosphorylation was normalized to PKCδ protein levels.

Peptide kinase assays were carried out in a similar manner in 200 μl of a reaction mixture containing 26 mM Tris, pH 7.5, 5 mM $MgCl_2$, 0.6 mM EGTA, 0.6 mM EDTA, 0.5 μM PKI, 10 μM protein phosphatase 1 (PP1), 0.25 mM DTT, 89 μg/ml phosphatidylserine plus 175 nM PMA, and 50 μM peptide substrate, as indicated in the legend of Fig. 6. Reactions were initiated by the addition [γ-^{32}P]ATP (10 μCi, 66 μM) and were performed in quadruplicate at 30°C for 15 min. Assays were terminated by placing samples on ice, which was followed by centrifugation at 1,500 × *g* for 10 min at 4°C. Forty microliters of each supernatant was spotted onto phosphocellulose filter papers (P-81), which were dropped immediately into water and washed (five times for 5 min), and radioactivity counts were determined.

Multiple-reaction monitoring (MRM) phosphorylation of PKCδ. WT-PKCδ and PKCδ-ΔC2 enzymes were heterologously overexpressed in HEK293 cells, immunoprecipitated for IVKAs, and then subjected to in-gel digestion as described previously (15). Briefly, WT-PKCδ and PKCδ-ΔC2 bands separated by SDS-PAGE were excised, cut into 1-mm pieces, and washed three times with 50% acetonitrile–25 mM ammonium bicarbonate for 15 min with shaking. Gel pieces were incubated with 25 mM ammonium bicarbonate plus 10 mM dithiothreitol for 60 min at 55°C, washed with acetonitrile (ACN), and then incubated with 25 mM ammonium bicarbonate plus 55 mM iodoacetamide (freshly made) for 30 min in the dark. Gel pieces were then washed with ACN, dried, rehydrated with 10 ng/μl trypsin (sequencing grade; Promega) in 25 mM ammonium bicarbonate, and then placed on ice for 30 min. Excess trypsin was removed, and then 20 μl of 25 mM ammonium bicarbonate was added. Samples were digested at 37°C for 18 h. The liquid was transferred to a clean tube. The peptides were extracted twice using 50% ACN–0.1% trifluoroacetic acid (TFA) for 20 min at 25°C with shaking. The final peptide mixture was subjected to C_{18} reverse-phase chromatography in C_{18} ZipTips (Millipore) using 0.1% TFA. The peptides were then eluted two times with 20 μl of 70% ACN–0.1% TFA and 95% ACN–0.1% TFA. The combined solution was dried using a SpeedVac vacuum centrifuge (Thermo Electron) and frozen at −80°C until analysis.

MRM assays were developed, optimized, and validated using a nano-liquid chromatography-tandem mass spectrometry (nano-LC-MS/MS) system, the 4000 QTRAP hybrid triple-quadrupole/linear ion trap mass spectrometer (AB Sciex). Peptides obtained from the in-gel digestion of PKCδ proteins were reconstituted in 20 μl of 0.1% formic acid. Peptides were separated by an Eksigent Tempo nano-LC system (Eksigent Technology) onto a BioBasic C_{18} reverse-phase PicoFrit column (300-Å pore size, 5-μm particle size, 75-μm inner diameter by 10-cm length, 15-μm tip; New Objective). Peptides were eluted in a 36-min AB linear gradient from 5 to 40% mobile phase B (mobile phase A, 2% [vol/vol] ACN containing 0.1% [vol/vol] formic acid; mobile phase B, 98% [vol/vol] ACN containing 0.1% [vol/vol] formic acid) at a 500 nl/min flow rate on the 4000 QTRAP MS system, with the NanoSpray source spray head coupled to a distal coated PicoTip fused silica spray tip (360-μm outside diameter, 75-μm inside diameter, 15-μm emitter orifice diameter; New Objective). Samples were analyzed using the following settings: curtain gas (CUR), 15; collision gas (CAD), high; ion spray voltage (IS), 2.5 kV; ion source gas 1 (GS1), 25; ion source gas 2 (GS2), 0; resolution Q1 and Q3, unit; heater interface temperature, 150°C. Each sample was run in triplicate. Peak detection and quantification of peak area were determined with Multiquant software, version 2.0, and inspected manually to ensure correct peak identification and quantification. Quantification of PKCδ phosphosites was carried out using a ratio of the peak area to gel band densitometry.

FRET sensor data. The C2 domain of PKCδ (123 aa) was cloned from full-length human PKCδ cDNA. All constructs contain an N-terminal Flag tag immediately followed by mCitrine. In sequence behind the

mCitrine are the C2 domain of PKCδ, 10-nm ER/K α-helix linker (16), a tobacco etch virus (TEV) protease site (ENLYFQ), mCerulean, and a 13-amino-acid peptide sequence containing a Tyr residue that when phosphorylated corresponds to a C2 domain consensus binding site. Fluorescent resonance energy transfer (FRET) sensors were generated with either the optimal binding sequence MALYSI**Y**QPYVFA (4), the native PKCδ SEPVGI**Y**^{313}QGFEKK sequence, or these sequences with Tyr→Phe (in boldface) substitutions (MALYSI**F**QPYVFA and SEPVGI**F**QGFEKK) as controls. All domains and fluorophores are linked with three to four Gly-Ser-Gly repeats to allow rotational flexibility and are cloned between unique restriction sites. A C2 domain H62D mutation was generated by site-directed mutagenesis (QuikChange; Stratagene). These constructs were cloned between unique restriction sites in pBiex-1 vector and used for expression in Sf9 cells. Proteins were purified as described previously (17). FRET spectra for recombinant proteins were acquired on a FluoroMax-4 fluorometer (Horiba Scientific). Samples were excited at 430 nm (spectral band pass [bp 8 nm]), and emission was scanned from 450 to 650 nm (bp 4 nm). All samples were suspended in a buffer composed of 50 mM Tris-HCl, 10 mM $MgCl_2$, 10% glycerol, and 2.5 mM DTT. Recombinant Src kinase was added to the reaction samples and incubated at 30°C for 30 min before spectra were taken. The samples also contain 0.05 mg/ml bovine serum albumin (BSA) to limit nonspecific surface adsorption of sensor proteins.

RESULTS

A FRET-based sensor detects a C2 domain interaction with a pTyr^{313}-bearing peptide. Since traditional bimolecular approaches are unlikely to be an effective approach to detect a *cis* interaction between the C2 domain and the pTyr^{313} motif (which is predicted to be facilitated by the tethering of the two domains within full-length PKCδ), we generated FRET-based sensors consisting of a single polypeptide with (N to C terminus) the C2 domain, mCerulean (as FRET donor), an ER/K linker (18), a 13-residue peptide based upon either a previously described optimal pTyr binding motif (4) or sequence flanking Tyr^{313} in PKCδ, and mCitrine (as a FRET acceptor). These sensors are designed to primarily report on the strength of the interaction between the C2 domain and the peptide (higher FRET indicates a stronger interaction) (Fig. 1A) (16). Sensors were purified and subjected to *in vitro* kinase assays with recombinant Src. Figure 1B and C show that the FRET signals for sensors bearing either the optimal pTyr binding motif or the Tyr^{313}-bearing peptide increase as a result of *in vitro* phosphorylation by Src. Two sets of control sensors were generated to establish the specificity of the FRET signals (Fig. 1C). First, studies with sensors containing Tyr→Phe substitutions at each peptide's phosphorylation site establish that the increase in FRET signal is due to phosphorylation at the designated tyrosine residue in the peptide. Second, studies with sensors containing H62D substitutions in the C2 domain pTyr binding pocket (that disrupts the C2 domain-pTyr interaction) (schematic in Fig. 1D) (4) point to a phosphorylation-dependent interaction with the C2 domain. These results indicate that the Src-dependent increases in FRET are due to C2 domain interactions with Tyr-bearing peptides, providing direct evidence for an interaction between the C2 domain and the pTyr^{313} motif in the V3 hinge of PKCδ.

The C2 domain is required for *in vivo* PMA-dependent PKCδ-Tyr^{313} phosphorylation. We used a PKCδ-C2 domain deletion construct (PKCδ-ΔC2) to examine the consequences of C2 domain-dependent interactions in a cellular context. Figure 2A shows that WT-PKCδ and PKCδ-ΔC2 are expressed at similar levels in HEK293 cells and that both enzymes undergo similar maturational phosphorylations at the activation loop (Thr^{507}) and C-terminal (Ser^{645} and Ser^{664}) phosphorylation sites. These "priming" site phosphorylations are stable modifications that are not altered by PMA or H_2O_2. H_2O_2 and pervanadate promote WT-PKCδ and PKCδ-ΔC2 phosphorylation at Tyr^{313} and Tyr^{334} (Fig. 2A and B). In each case, Tyr^{313} and Tyr^{334} phosphorylation is via an Src-dependent mechanism that is inhibited by PP1 (7). In contrast, PMA induces an Src-dependent increase in WT-PKCδ phosphorylation at Tyr^{313} but not at Tyr^{334}. PMA does not increase PKCδ-ΔC2 phosphorylation at Tyr^{313} (Fig. 2A and B).

Control studies indicate that the effect of the C2 domain deletion to prevent PMA-dependent Tyr^{313} phosphorylation is not due to a defect in PKCδ targeting to Src-enriched caveolar membranes. Figure 2C shows that WT-PKCδ and PKCδ-ΔC2 both translocate to the caveolar membrane fraction. These results indicate that some other mechanism must account for the selective defect in PMA-dependent PKCδ-ΔC2-Tyr^{313} phosphorylation. Therefore, we considered whether a C2 domain deletion disrupts the docking interaction that protects the phosphorylation site at Tyr^{313} (but not Tyr^{334}) from dephosphorylation by cellular phosphatases. This mechanism could account for the puzzling observation that Src phosphorylates PKCδ *in vitro* at both Tyr^{313} and Tyr^{334} although PKCδ is phosphorylated via an Src-dependent mechanism at Tyr^{313} and not Tyr^{334} in PMA-treated cells. Indeed, Fig. 2D shows that a PKCδ H62D substitution in the C2 domain pY binding site (4) completely abrogates PMA-dependent Tyr^{313} phosphorylation, whereas Tyr^{313} phosphorylation is not influenced by a Y64F substitution at an adjacent site in the C2 domain that does not contribute to pY binding.

PKCδ-ΔC2 displays a high level of cTnI-Thr^{144} and cTnT kinase activity that is not influenced by Src. We performed *in vitro* kinase assays (IVKAs) without and with Src in buffers containing [γ^{32}P]ATP, PS/PMA, and cardiac troponin (cTn) complex (consisting of equimolar cTnI, cardiac troponin T [cTnT], and cardiac troponin C [cTnC] as the substrate) to determine whether a C2 domain deletion alters PKCδ's *in vitro* enzymology. Figure 3 shows that WT-PKCδ executes a time-dependent autophosphorylation reaction. This is tracked as an increase in ^{32}P incorporation, which provides an integrated measure of autophosphorylation and (where specified) PKCδ tyrosine phosphorylation by Src (Fig. 3); a representative autoradiogram is depicted on the left, with the results of three separate experiments quantified on the right. PKCδ autophosphorylation also is detected by immunoblot analysis with an anti-pTXR motif phosphorylation site-specific antibody (PSSA) that specifically recognizes one of several autophosphorylation sites on PKCδ at Thr^{295} (19). It is important to note that Thr^{295} autophosphorylation is tracked in this study solely as a convenient readout of PKCδ autocatalytic activity. Studies to date show that a T295A substitution (in the vicinity of Tyr^{313}) leads to a defect in Src-dependent PKCδ-Tyr^{313} phosphorylation (and therefore prevents the Src-dependent increase in PKCδ catalytic activity) but that a T295A substitution does not otherwise grossly influence PKCδ catalytic activity. Insofar as this study focuses on mechanisms that activate PKCδ downstream from Src (that bypass the requirement for phosphorylation at Tyr^{313}) (see below), a regulatory role for Thr^{295} autophosphorylation is unlikely and was not considered. Figure 3 shows that WT-PKCδ executes a time-dependent autophosphorylation and that autophosphorylation (quantified as ^{32}P incorporation) is enhanced by Src, consistent with previous evidence that Src enhances PKCδ's autocatalytic activity.

The kinetics of PKCδ phosphorylation of cTnI and cTnT were

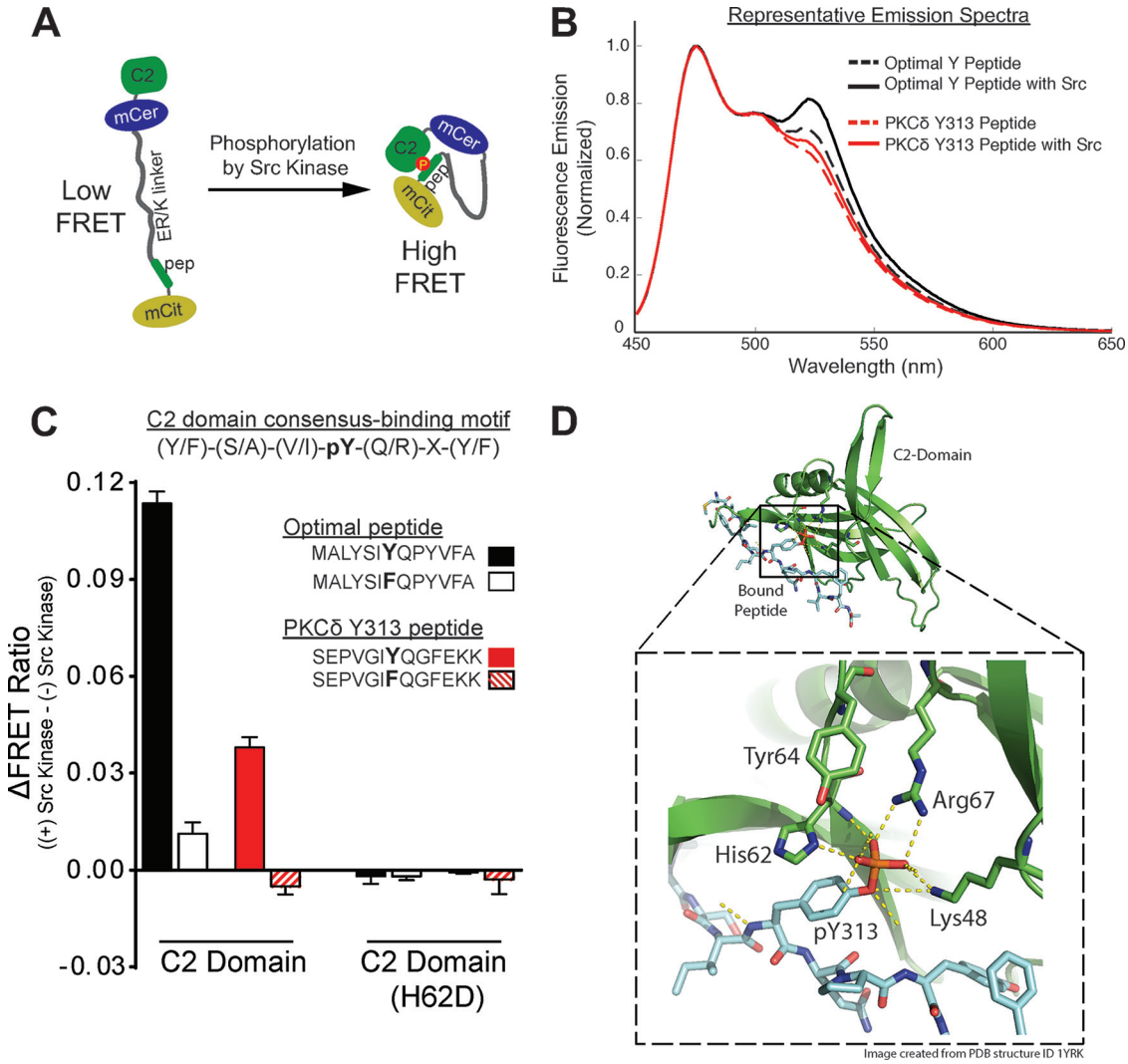

FIG 1 A FRET-based sensor detects a C2 domain interaction with PKCδ's pTyr^{313} motif. (A) Schematic of the C2 domain pY peptide-binding motif sensor in the unphosphorylated/inactive (left) and phosphorylated/active (right) conformations. The sensor consists of a single polypeptide containing (from its N to C terminus) the C2 domain, mCerulean (mCer), an ER/K α-helical linker, a peptide based upon the optimal C2 domain peptide binding motif previously defined by Benes et al. (4) or sequence flanking the Tyr^{313} site in PKCδ, and mCitrine (mCit). (B) Representative emission spectra, after donor excitation at 430 nm, of indicated sensors before and after treatment with Src kinase (donor emission peak, 475 nm; acceptor emission peak, 525 nm). (C) Src-dependent changes in the FRET ratio (mCitrine/mCerulean, 525 nm/475 nm) for wild-type and mutant sensors. Data are means ± standard deviations of at least four spectral repeats. Results were consistent in three independent recombinant sensor preparations. (D) Schematic representation of the interface between the pY^{313} peptide (cyan backbone) and the C2 domain (green ribbon) of PKCδ (modeled on Protein Data Bank [PDB] accession number 1YFK). Residues that contribute to pTyr-binding (Lys^{48}, Arg^{67}, and His^{62}) and Tyr^{64} at the binding interface are highlighted in the bottom inset.

examined in parallel (note that cTnC is not a substrate for PKC). Figure 3 shows that the time course for WT-PKCδ phosphorylation of individual sites on cTnI is strikingly different. WT-PKCδ phosphorylates cTnI at Ser^{23}/Ser^{24} very rapidly. This reaction reaches a maximal level at early time points, well in advance of WT-PKCδ-Thr^{295} autophosphorylation or WT-PKCδ-Tyr^{313} phosphorylation by Src. In contrast, WT-PKCδ phosphorylation of cTnI at Thr^{144} is detected following more prolonged incubations (30 to 60 min) exclusively in assays with Src. The anti-pTXR motif PSSA also exposes an Src-dependent increase in PKCδ phosphorylation of cTnT; cTnT contains three TXR motifs (in boldface) in PKC phosphorylation clusters at **T^{194}ER**KS^{198}GKRQ**T^{203}ER** and KV**T^{284}GR**. Importantly, we previously showed that the Src-dependent acquisition of cTnI-Thr^{144} kinase activity is abrogated by a Y313F substitution in PKCδ (9); a Y313F substitution also abrogates the Src-dependent increase in TXR motif phosphorylation on cTnT (data not shown).

A similar kinetic analysis of the *in vitro* kinase activity of PKCδ-ΔC2 shows the following. (i) PKCδ-ΔC2 exhibits a time-dependent increase in autophosphorylation, detected as an increase in ^{32}P incorporation and phosphorylation at Thr^{295}. Quantification, based upon ^{32}P incorporation, shows that PKCδ-ΔC2 autophosphorylates to a higher level than WT-PKCδ; PKCδ-ΔC2 autophosphorylation is not influenced by Src. (ii) PKCδ-ΔC2 phosphorylates cTnI at Ser^{23}/Ser^{24} but, unlike WT-PKCδ, displays a high level of Src-independent cTnI-Thr^{144} and cTnT-TXR motif activity. These results suggest that the C2 domain functions to limit PKCδ-dependent cTnI-Thr^{144} and cTnT-TXR motif phosphorylation.

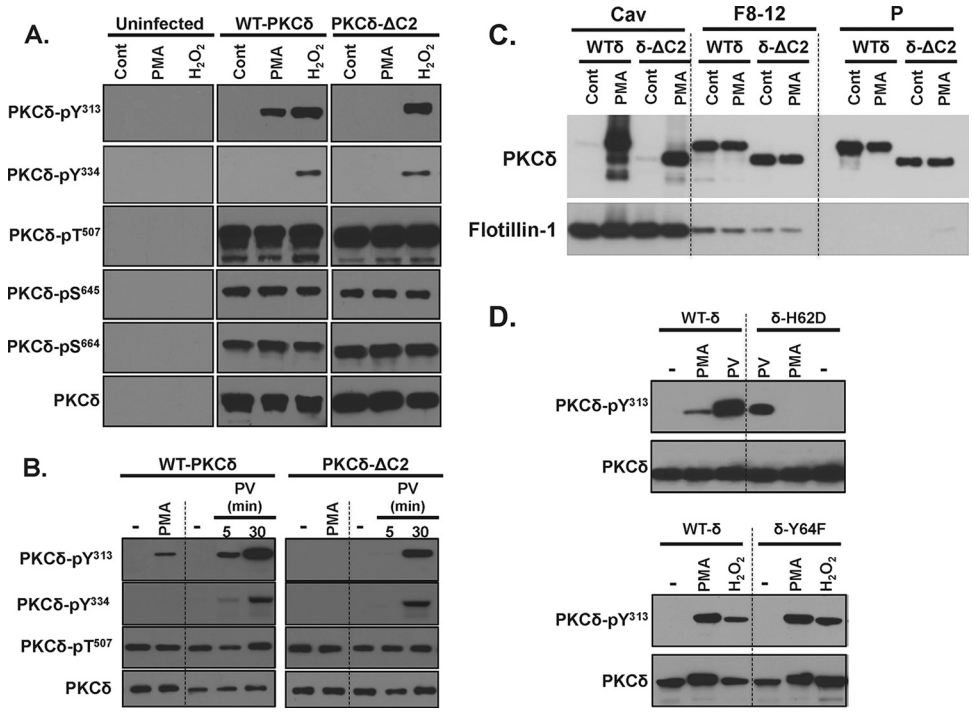

FIG 2 PMA-dependent PKCδ-Tyr^{313} phosphorylation requires an intact pTyr-binding C2 domain. HEK293 cells that transiently overexpress WT-PKCδ (WT-δ) and PKCδ-ΔC2 (δ-ΔC2) (A to C) or PKCδ-H62D (δ-H62D) or PKCδ-Y64F (δ-Y64F) (D) were challenged with vehicle, 300 nM PMA, 5 mM H_2O_2, or 100 μM pervanadate (PV) as indicated. Immunoblotting was on cell lysates (A, B, and D) or on the caveolar fraction (Cav), pooled heavy gradient fractions (F8 to F12), and the insoluble pellet (P) that are separated by a detergent-free caveolar purification scheme (C). It should be noted that the bands representing WT-PKCδ and PKCδ-ΔC2 were aligned for presentation purposes in panels A and B; the increased electrophoretic mobility due to the C2 domain deletion was observed in all experiments and can be observed in panel C. All results were replicated in three to six separate experiments on separate culture preparations. Each panel shows results from a single gel exposed for a uniform duration.

The C2 domain controls phosphorylation of the ATP-positioning loop at Ser^{359}. WT-PKCδ and PKCδ-ΔC2 were subjected to IVKAs and then targeted multiple-reaction monitoring (MRM)–mass spectrometry to determine whether PKCδ-ΔC2's altered enzymology is attributable to a change in phosphorylation. We identified a novel phosphorylation site at Ser^{359} in the highly conserved Gly-rich ATP-positioning loop (G loop, also known as the phosphate positioning P loop) in the small lobe of the kinase domain (see Fig. S1 in the supplemental material). Quantification (peak areas) showed that the Ser^{359}-phosphorylated peptide is detected by MRM in tryptic digests from WT-PKCδ but that it is not detected in digests from PKCδ-ΔC2 (see Fig. S1A, B, E, and F in the supplemental material). The precise stoichiometry of phosphorylation at this site could not be assessed since unphosphorylated Ser^{359} peptide ionizes poorly in the MS instrument; it is detected (elution time, ~16 min), but the levels are below the lower limit of quantification.

We developed an anti-PKCδ-pSer^{359} PSSA as a separate strategy to track PKCδ G-loop phosphorylation. Figure 3B shows the validation of this reagent; the anti-PKCδ-pSer^{359} PSSA recognizes WT-PKCδ but not a PKCδ-S359A mutant. Western blots using this reagent show that Ser^{359} phosphorylation is detected on WT-PKCδ but not on the PKCδ-ΔC2 mutant (Fig. 3B). Separate experiments showed that WT-PKCδ or PKCδ-ΔC2 phosphorylation at Ser^{359} does not grossly change during the IVKA (data not shown). This contrasts with phosphorylation at Thr^{295}, which increases during IVKAs on both WT-PKCδ and PKCδ-ΔC2 (Fig. 3A). The Thr^{295}-phosphorylated peptide also was detected in the MRM studies, where the quantification showed a 37% higher level of the Thr^{295}-phosphorylated peptide in tryptic digests from PKCδ-ΔC2 than in the digest from WT-PKCδ (see Fig. S1A to D in the supplemental material).

The C2 domain regulates PKCδ catalytic activity indirectly by controlling Ser^{359} phosphorylation. PKCδ mutants harboring single-residue substitutions at position 359 (either on the WT-PKCδ or PKCδ-ΔC2 backbone) were subjected to IVKAs to examine their autocatalytic and Tn kinase activities. Preliminary studies showed that Ser^{359} substitutions do not grossly alter PKCδ expression, priming site (Thr^{507}, Ser^{645}, and Ser^{664}) phosphorylation, or cTnI-Ser^{23}/Ser^{24} kinase activity (data not shown), suggesting that the PKCδ G loop is a relatively flexible structure that accommodates a range of amino acid substitutions at position 359.

Figure 4 shows that WT-PKCδ activity is strictly lipid dependent, but PKCδ-S359A possesses a considerable amount of lipid-independent autocatalytic activity, detected as a high level of lipid-independent autophosphorylation at Thr^{295} (Fig. 4A) and ^{32}P incorporation (Fig. 4B). The S359A substitution also increases lipid-independent cTnI-Ser^{23}/Ser^{24} kinase activity (relative to WT-PKCδ), and it confers Src-independent cTnI-Thr^{144} and cTnT-TXR kinase activity. PS/PMA treatment results in further increases in PKCδ-S359A activities.

PKCδ-S359E also possesses a modest level of lipid-independent autocatalytic activity (detected as increased Thr^{295} autophos-

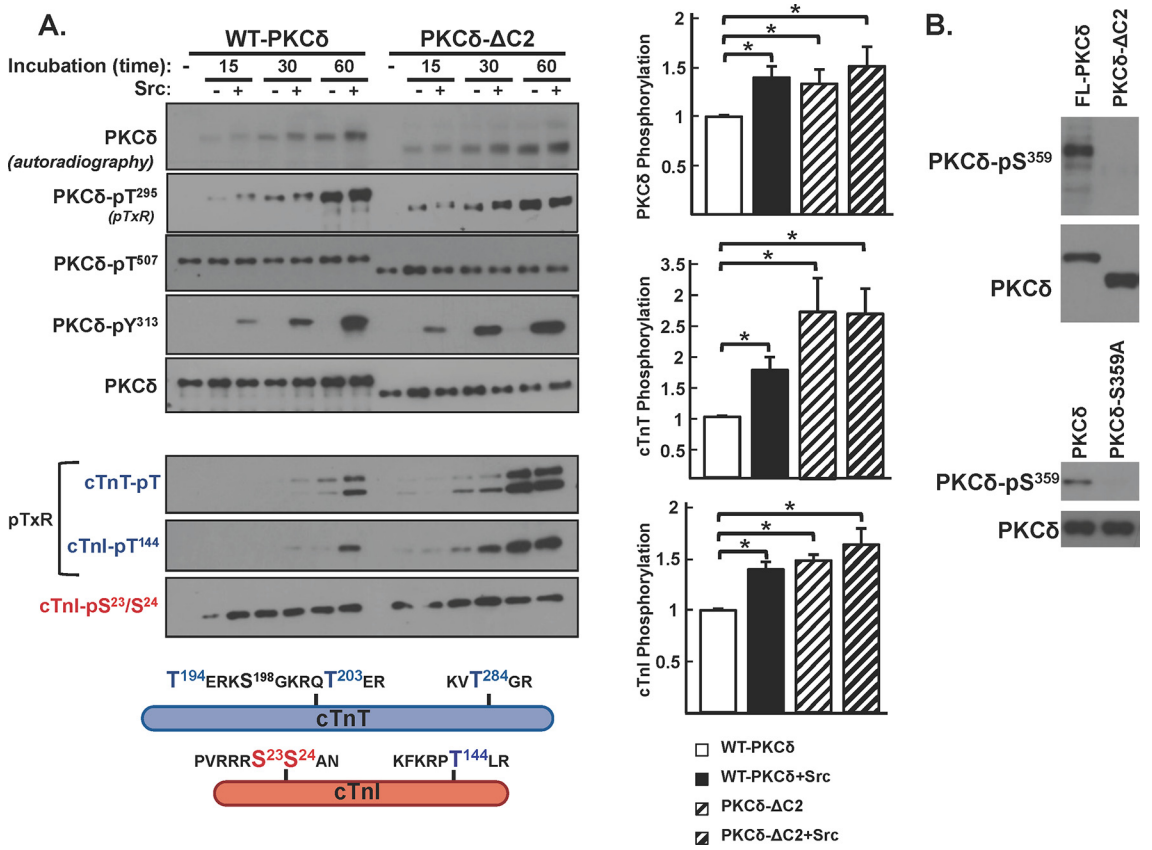

FIG 3 A C2 domain deletion confers Src-independent cTnI-Thr^{144} and cTnT kinase activity. (A) WT-PKCδ or PKCδ-ΔC2 was immunoprecipitated from HEK293 cells and subjected to IVKAs with PS/PMA with or without Src and Tn complex as the substrate. Autoradiography and immunoblotting were performed for PKCδ protein (to validate equal protein recovery) and PKCδ autophosphorylation at Thr^{295} and PKCδ-Tyr^{313} phosphorylation by Src (top left). Src also induces parallel increases in WT-PKCδ and PKCδ-ΔC2 phosphorylation at Tyr^{334}; these immunoblots have been omitted from the figure since we previously demonstrated that Tyr^{334} phosphorylation does not contribute to the control of PKCδ catalytic activity (9). Immunoblotting was performed for cTnI phosphorylation at Ser^{23}/Ser^{24}, cTnI phosphorylation at Thr^{144} (detected with an anti-pTXR motif PSSA) (9), and cTnT phosphorylation at TXR motifs (bottom left). The schematic shows PKC phosphorylation sites on cTnI and cTnT. Results for ^{32}P incorporation into PKCδ, cTnI, and cTnT are quantified ($n = 3$) (right). Results in each panel are normalized to phosphorylation levels detected in assays with WT-PKCδ activity. Results are presented as the means ± standard errors and are analyzed with a Student's t test with a Bonferroni correction for multiple comparisons (*, $P < 0.05$). (B) WT-PKCδ, PKCδ-ΔC2, or PKCδ-S359A was immunoprecipitated from HEK293 cells and subjected to immunoblot analysis with a PSSA that specifically recognizes phosphorylation at Ser^{359} or PKCδ protein (to validate equal protein loading).

phorylation and ^{32}P incorporation into the enzyme) (Fig. 4A and B). The observation that S→E and S→A substitutions both increase lipid-independent PKCδ autocatalytic activity suggests that an electrostatic interaction involving the Ser^{359} hydroxyl group (rather than Ser^{359} phosphorylation) stabilizes the inactive conformation of the enzyme. However, S359A and S359E substitutions exert very different effects on Tn phosphorylation. PKCδ-S359E retains wild-type cTnI-Ser^{23}/Ser^{24} kinase activity, but it does not phosphorylate cTnI at Thr^{144} or cTnT at TXR motifs (even when it is Tyr^{313} phosphorylated by Src). While a PKCδ-S359E-dependent increase in ^{32}P incorporation into cTnT was detected in assays with Src (Fig. 4B), this was mapped to a different cTnT phosphorylation site that is recognized by an anti-PKC substrate motif PSSA (that recognizes pS flanked by R or K at −2 and +2 positions) (Fig. 4A); cTnT's PKC phosphorylation cluster contains a site (T^{194}E**R**K**S^{198}**G**K**RQT^{203}ER; the phosphorylation site is underlined, and the boldface R at the −2 position and K at the +2 position relative to the phosphorylation site show that this conforms to the described PKC consensus motif) that conforms to this motif.

The antithetical effects of S359A and S359E substitutions on PKCδ's TXR kinase activity could suggest a role for a negative charge (e.g., phosphorylation) at this site. However, Fig. 4C shows that a position 359 bulky/uncharged Leu substitution also abrogates cTnI-Thr^{144} and cTnT-TXR motif phosphorylation, without disrupting PKCδ autocatalytic activity or cTnI-Ser^{23}/Ser^{24} kinase activity. These results argue that the steric bulk of a position 359 phosphate group (rather than the negative charge) disrupts PKCδ activity toward cTnI-Thr^{144} and cTnT-TXR motifs.

We introduced an S359E substitution into the PKCδ-ΔC2 backbone to test whether the C2 domain controls PKCδ catalytic activity indirectly by regulating Ser^{359} phosphorylation. Figure 4D shows that PKCδ-ΔC2 and PKCδ-ΔC2-S359E display similar cTnI-Ser^{23}/Ser^{24} kinase activities. PKCδ-ΔC2 (which is not detectably phosphorylated at Ser^{359}) displays high levels of cTnI-Thr^{144} and cTnT-TXR motif activity. cTnI-Thr^{144} and cTnT-TXR motif phosphorylation is completely abrogated by an S359E substitution in the PKCδ-ΔC2 backbone.

These studies (summarized in Fig. 5) implicate Ser^{359} as a novel PKCδ phosphorylation site that plays a heretofore unrecognized

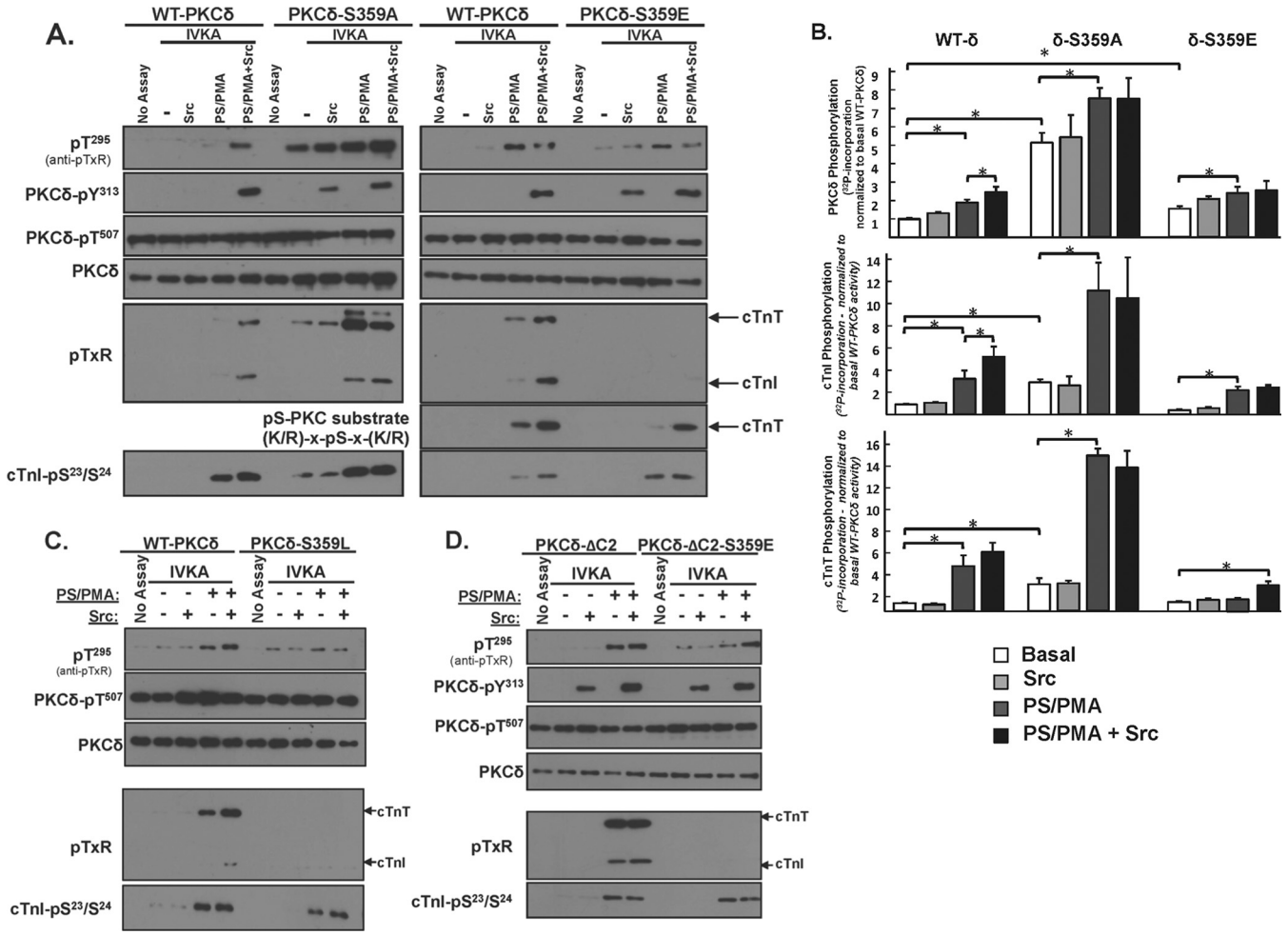

FIG 4 An S359A substitution enhances while an S359E substitution prevents cTnI and cTnT phosphorylation at TXR motifs. PKCδ constructs (WT-PKCδ, PKCδ-S359A, or PKCδ-S359E in panel A, PKCδ-S359L in panel C, and PKCδ-ΔC2 or PKCδ-ΔC2-S359E in panel D) were subjected to IVKAs with Tn complex as the substrate, without or with PS/PMA or Src as indicated. Phosphorylation was tracked by immunoblotting, with results representative of immunoblots from two (for PKCδ-S359L and PKCδ-ΔC2), three (for PKCδ-S359E), four (for PKCδ-S359A), or seven (for WT-PKCδ) separate experiments. (B) ^{32}P incorporation was quantified by phosphorimager analysis for assays performed with WT-PKCδ ($n = 7$), PKCδ-S359A ($n = 4$), and PKCδ-S359E ($n = 3$). Results are presented as the means ± standard errors and are analyzed with Student's *t* test with a Bonferroni correction for multiple comparisons (*, $P < 0.05$). Note that the apparent difference between the PS/PMA-dependent increases in WT-PKCδ-Thr^{295} phosphorylation in the two IVKAs in panel A is attributable to a difference in exposure times: optimal exposure times were considerably shorter for studies that compared WT-PKCδ with the highly active PKCδ-S359A mutant than for studies that compared WT-PKCδ with PKCδ-S359E (which have more similar autocatalytic activities).

role to control phosphorylation of TXR motifs on cTnI and cTnT (but not cTnI phosphorylation at Ser^{23}/Ser^{24}). However, these newer results also raise a question regarding the mechanism underlying our original observation that Src increases WT-PKCδ's *in vitro* TXR activity; Src-phosphorylated WT-PKCδ acquires TXR activity without any gross change in its Ser^{359} phosphorylation status in the IVKAs (an artificial context that does not include cellular phosphatases). The simplest, most parsimonious, explanation for this finding is that WT-PKCδ TXR activity arises from a pool of enzyme that is recovered without G-loop Ser^{359} phosphorylation. This formulation is consistent with (i) the MRM-MS studies that detected, but could not quantify, the unphosphorylated Ser^{359} peptide and (ii) the mutagenesis studies showing that TXR activity is completely abrogated by the phosphomimetic or bulky Ser^{359} substitutions, indicating that an unphosphorylated, or alanine substituted, Ser^{359} in the G loop is necessary for TXR activity. In fact, the data shown in Fig. 3 showing that WT-PKCδ displays a very low level of Src-independent TXR activity when incubations are pushed to very prolonged intervals suggest that TXR activity reflects both the fraction of total enzyme that is recovered without Ser^{359} phosphorylation and its overall catalytic activity and that Src increases WT-PKCδ's TXR activity by enhancing its catalytic activity (independent of any effect on Ser^{359} phosphorylation). We performed additional studies with the PKCδ-Y313F mutant enzyme (which prevents phosphorylation by Src but does not influence G-loop Ser^{359} phosphorylation) (see Fig. 8C) to test this hypothesis. The observation that a Y313F substitution decreases PKCδ autophosphorylation at Thr^{295} (53% ± 7% relative to WT-PKCδ; $P < 0.05$, $n = 3$) indicates that an Src-driven conformational change, which may or may not involve the C2 domain-pTyr^{313} docking interaction, contributes to the mechanism for maximal activation of WT-PKCδ.

An S359A substitution influences the phosphoacceptor preference of PKCδ. While PKCδ is generally viewed as an Ser/Thr

PKC-δ	cTnI		cTnT (*pT*)
	cTnI-pS^{23}/S^{24}	cTnI-pT^{144}	
WT-PKCδ	+	-	-
WT-PKCδ + Src	+	+	+
PKCδ-ΔC2	+	++	++
PKCδ-ΔC2-S359E	+	-	-
PKCδ-S359A	+	+++	+++
PKCδ-S359E (with or without Src)	+	-	-
PKCδ-S359L (with or without Src)	+	-	-

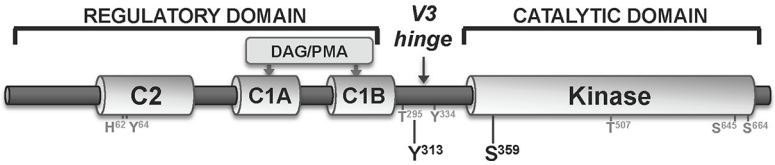

FIG 5 Summary of the PKCδ mutants used in this study and their activity toward phosphorylation sites on cTnI and cTnT. Regulatory phosphorylation sites at Y^{313} and S^{359}, priming phosphorylation sites (T^{507}, S^{645}, and S^{664}), and other residues examined in this study are localized in the schematic of the PKCδ domain structure.

kinase, substrate sequence logos suggest a clear preference for substrates with an Ser at the phosphoacceptor site (P site). Of note, structural studies of PKA complexed with ATP and PKI (an inhibitor peptide that docks to the active site) place the Ser in the GK GSFG sequence at the tip of the G loop in close proximity to the P site on substrates (Fig. 6A). Our observation that an S359A substitution (at the tip of the G loop of PKCδ) selectively increases phosphorylation of TXR (Thr-directed) motifs on cTnI and cTnT provided a rationale to test whether posttranslational modifications (PTMs) at Ser^{359} specifically regulate substrate phosphorylation at Thr (but not Ser) residues. We compared WT-PKCδ and PKCδ-S359A activity toward short peptide substrates based upon the cTnI phosphorylation site at position 144 with either Thr or Ser at the P site. It is worth noting that IVKAs described in the previous sections tracked WT-PKCδ phosphorylation of proteins in the troponin complex; these assays are performed at limiting/submicromolar substrate concentrations since practical issues related to cost and protein insolubility preclude the use of higher concentrations of protein substrates. In contrast, peptide kinase assays are performed at a considerably higher substrate concentration (50 μM) and expose a low level of cTnI-Thr^{144} phosphorylation by PKCδ. However, Fig. 6B shows that WT-PKCδ displays a considerably higher level of activity toward the cTnI-Ser^{144} peptide. Moreover, the S359A substitution increases peptide kinase activity. PKCδ-S359A phosphorylates both cTnI-Thr^{144} and cTnI-Ser^{144} peptides; it does not discriminate between these peptides. Similar results were obtained in assays with peptides based upon the Ser^{133} phosphorylation site in CREB, which is flanked by a different phosphorylation motif (Fig. 6C). In this case, WT-PKCδ and PKCδ-S359A display high levels of activity toward the CREB-Ser^{133} peptide. An S133T substitution markedly decreases peptide phosphorylation by WT-PKCδ but not PKCδ-S359A. These results implicate PTMs at Ser^{359} in PKCδ's G loop as a mechanism that regulates PKCδ's P-site specificity.

G-loop regulation of PKCα and PKA activities. The G-loop Ser^{359} phosphorylation site in PKCδ is highly conserved in other PKCs and in PKA (Fig. 7). Since there is recent evidence that this G-loop site is posttranslationally modified in PKCα and PKA (20, 21) and since the functional role of this site in PKCα and PKA remains uncertain, we examined whether G-loop substitutions influence PKCα or PKA catalytic activity. Figure 7B and C show that single-residue substitutions in the G-loops of PKCα (at Ser^{349}) or PKA (at Ser^{53}) do not influence enzyme expression or priming/activation loop phosphorylation. WT-PKCα displays a modest amount of activity toward cTnI-Ser^{23}/Ser^{24} in assays with PS/PMA (Fig. 7B). The S349A substitution increases PKCα's lipid-dependent cTnI-Ser^{23}/Ser^{24} kinase activity, without imparting activity toward cTnI-Thr^{144} or cTnT-TXR motifs (and it does not confer lipid-independent catalytic activity). Control studies performed in parallel show that a similar level of cTnI-Ser^{23}/Ser^{24} phosphorylation by lipid-/Src-activated PKCδ is associated with considerable amounts of cTnI-Thr^{144} and cTnT-TXR activity. Figure 7C shows that an S53A substitution increases while an S53E substitution decreases cTnI-Ser^{23}/Ser^{24} phosphorylation by PKA. WT and mutant PKA constructs do not phosphorylate TXR sites on cTnI or cTnT. Collectively, these studies implicate G-loop

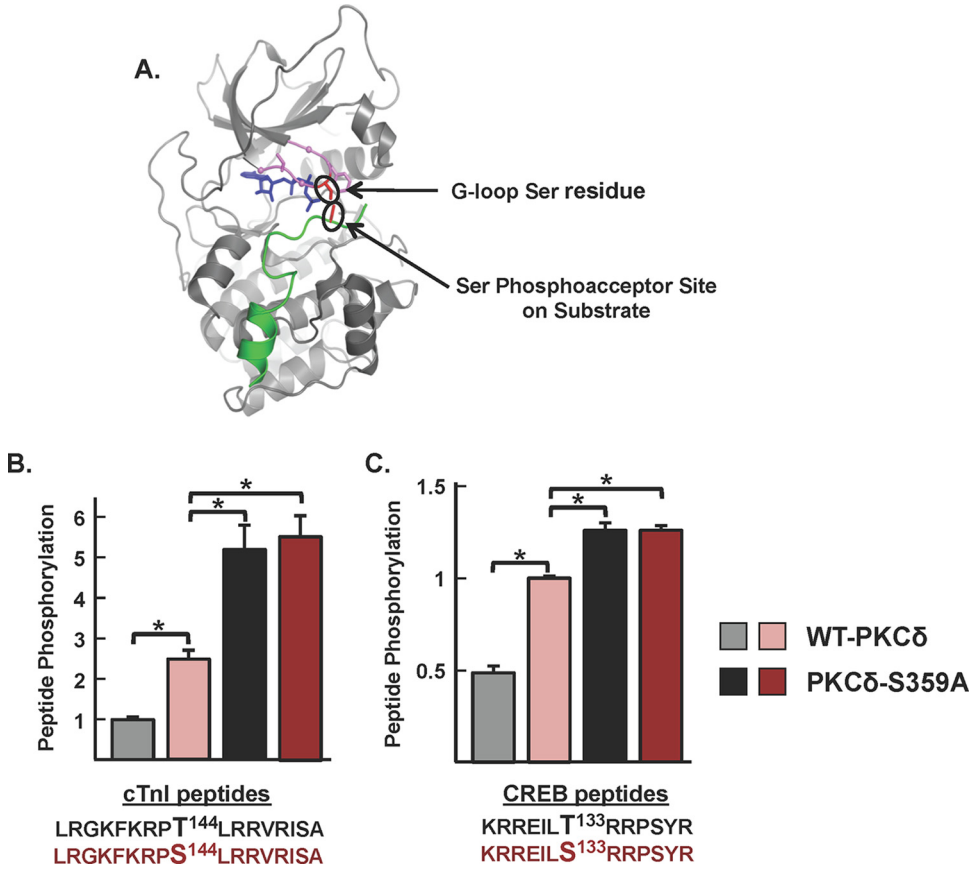

FIG 6 The ATP binding loop Ser[359] phosphorylation site controls P-site selectivity. (A) Structure of the PKA catalytic subunit (PDB accession number 3FJQ) complexed with PKI (in green) and ATP (in blue) at the cleft interface. The Gly-rich loop (GKGSFG) is highlighted in violet, with α-carbons of the three Gly residues shown as balls. Side chains of the G-loop Ser and Phe residues are included, with the G-loop Ser residue highlighted in red. The Ser residue at the P site of PKI also is highlighted in red. The close-up view of the G-loop region of the PKA-PKI-ATP ternary complex shows the close proximity between the Ser residue at the tip of the G loop and the phosphoacceptor site on substrate. The PKA structure is depicted since there are no structural data for a PKC isoform complexed with ATP and substrate. (B and C) WT-PKCδ and PKCδ-S359A phosphorylation of peptide substrates with either Thr or Ser at the position 144 phosphorylation site in cTnI (B) or the position 133 phosphorylation site in CREB (C) was examined in triplicate, as described in Materials and Methods. Results are presented as the means ± standard errors from three separate experiments (*, $P < 0.05$).

PTMs as general regulators of PKCδ, PKCα, and PKA activity. In each case, S→A substitutions increase and S→E substitutions decrease activity. However, the detailed nature of the regulatory control is kinase specific. The G-loop S→A substitution confers TXR motif activity on PKCδ but not on PKCα or PKA.

H_2O_2 decreases PKCδ-Ser[359] phosphorylation in cardiomyocytes; PKCδ-S359A displays an activated phenotype in cardiomyocytes. We examined whether PKCδ-Ser[359] phosphorylation is regulated in cardiomyocytes. Figure 8A shows that endogenous PKCδ is recovered from cardiomyocytes as a Ser[359]-phosphorylated enzyme and that PKCδ-Ser[359] phosphorylation decreases in association with the H_2O_2-dependent increase in PKCδ phosphorylation at Tyr[313]. PKCδ-pSer[359] immunoreactivity is reduced by 74% ± 4% relative to levels in resting cardiomyocytes following treatment with 5 mM H_2O_2 ($n = 4$, $P < 0.05$). Figure 8B shows that the reciprocal H_2O_2-dependent changes in PKCδ-Tyr[313] and Ser[359] phosphorylation are associated with the acquisition of lipid-independent cTnI-Ser[23]/Ser[24] and cTnI-Thr[144] kinase activities. Figure 8C uses a heterologous overexpression strategy to establish a link between the H_2O_2-dependent changes in Tyr[313] and Ser[359] phosphorylation. Figure 8C shows that the H_2O_2-dependent decrease in Ser[359] phosphorylation is abrogated by a Y313F substitution.

We used an overexpression strategy with WT-PKCδ and PKCδ-S359A followed by immunoblotting with the anti-PKC substrate PSSA (as a general screen for target protein phosphorylation), anti-pTXR (a specific screen for phosphorylation at Thr phosphoacceptor sites), and antibodies that recognize activating phosphorylations on protein kinase D (PKD, a PKCδ-activated effector) (22) to examine the functional importance of Ser[359] in a cellular context. Immunoblotting studies on cell lysates show that WT-PKCδ or PKCδ-S359A overexpression leads to an increase in PMA-dependent responses (Fig. 8D). However, PKCδ-S359A uniquely acts as a constitutively activated enzyme to enhance (basal) anti-PKC substrate PSSA immunoreactivity and phosphorylation/activation of PKD (Fig. 8D). PKCδ-S359A overexpression also increases substrate phosphorylation at TXR motifs. However, pTXR motif immunoreactivity was detected on only a limited number of proteins in cell lysates. Therefore, we also assessed phosphorylation in the myofibrillar fraction. Figure 8D shows that WT-PKCδ and PKCδ-S359A overexpression leads to a marked increase in basal and PMA-dependent anti-

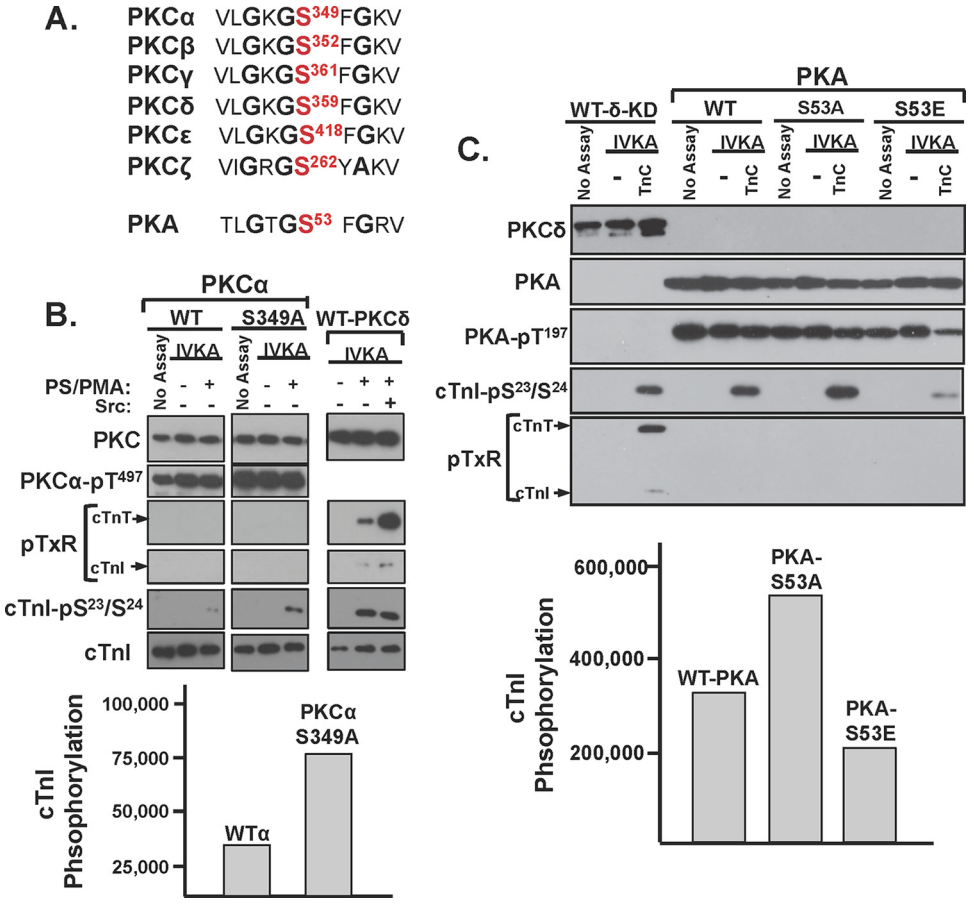

FIG 7 S→A substitutions in the G loops of PKCα and PKA increase cTnI-Ser^{23}/Ser^{24} phosphorylation without conferring activity toward cTnI-Thr^{144} or TXR sites on cTnT. (A) Alignment of the highly conserved G loops in PKC isoforms and PKA. WT-PKCα and PKCα-S349A (B) or WT-PKA, PKA-S53A, and PKA-S53E (C) were subjected to IVKAs with Tn complex (TnC) as the substrate. Control experiments were performed in parallel with full-length WT-PKCδ (with and without PS/PMA and Src added, as indicated) (B) or a PKCδ isolated kinase domain (KD) construct (C). Protein expression, activation loop (PKCα-Thr^{497} or PKA-Thr^{197}) phosphorylation, and substrate phosphorylation were tracked by immunoblot analysis (top panels); ^{32}P incorporation into cTnI was quantified by phosphorimager (bottom panels). All results were replicated in two separate experiments. WTα, WT-PKCα.

PKC substrate PSSA immunoreactivity in the myofibrillar fraction: PKC substrate motif phosphorylation is higher in cardiomyocytes that overexpress PKCδ-S359A than in cardiomyocytes that overexpress WT-PKCδ. The myofibrillar fractions also contain considerable amounts of pTXR immunoreactivity. pTXR immunoreactivity (including on a band that comigrates with cTnT) is considerably higher in the myofibrillar fraction from cardiomyocytes that overexpress PKCδ-S359A than in WT-PKCδ.

DISCUSSION

PKCδ was originally described as a signaling kinase that mediates growth factor-dependent cellular responses. The original allosteric model of PKCδ activation focused on translocation events that deliver the enzyme in an active conformation to DAG-enriched membranes. This model assumes that the cellular actions of PKCδ are membrane delimited and that PKCδ's catalytic activity is an inherent property of the enzyme that is not altered by the activation process. However, subsequent studies exposed alternative lipid-independent mechanisms for PKCδ activation that result in the generation of distinct molecular forms of PKCδ with altered catalytic properties in various subcellular compartments (not just in DAG-enriched membranes). We previously reported that oxidative stress leads to the activation of Src and accumulation of a Tyr^{313}-phosphorylated form of PKCδ with altered catalytic properties in cardiomyocytes (7, 9). This study identifies the mechanism that links Tyr^{313} phosphorylation to changes in catalytic activity by showing that the Tyr^{313}-phosphorylated hinge region functions as a docking site for the pTyr binding C2 domain of PKCδ (schematized in Fig. 9).

We used a PKCδ-ΔC2 deletion mutant to examine the functional consequences of C2 domain-mediated docking interactions. First, we showed that full-length PKCδ phosphorylates cTnI-Thr^{144} and cTnT-TXR motifs when it is Tyr^{313} phosphorylated by Src. In contrast, PKCδ-ΔC2 possesses a high level of Src-independent cTnI-Thr^{144} and cTnT-TXR motif activity. These results suggest that the C2 domain functions as an autoinhibitory regulator of certain full-length PKCδ activities and that a docking interaction between the C2 domain and the Tyr^{313}-phosphorylated hinge region induces a global conformational change that relieves this C2 domain-mediated autoinhibitory constraint. Second, we showed that the C2 domain regulates PKCδ activity by controlling phosphorylation at Ser^{359}. WT-PKCδ displays a high level of Ser^{359} phosphorylation. Studies

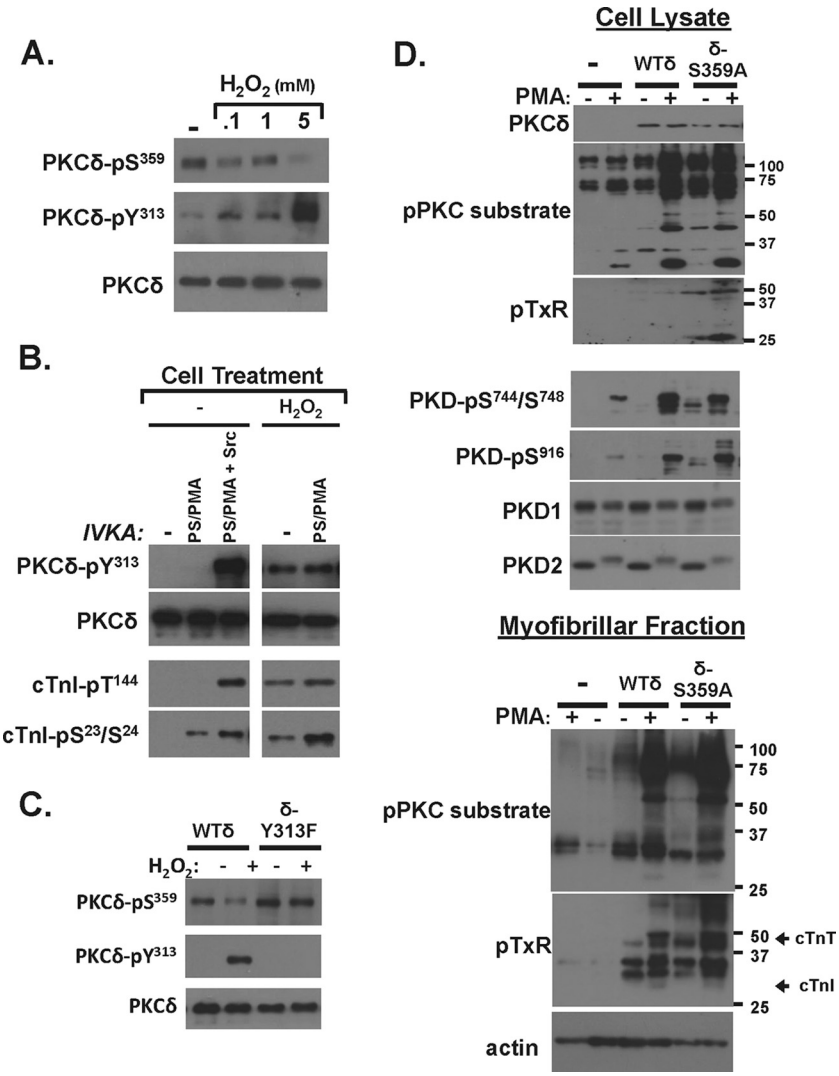

FIG 8 H_2O_2 decreases PKCδ-Ser^{359} phosphorylation in cardiomyocytes; PKCδ-S359A displays an activated phenotype in cardiomyocytes. (A and B) Neonatal rat cardiomyocyte cultures were treated for 5 min with vehicle or the indicated concentrations of H_2O_2. Endogenous PKCδ was then immunoprecipitated and probed for phosphorylation at Tyr^{313} and Ser^{359} (A) or subjected to IVKAs to track basal and lipid-dependent activity toward individual sites on cTnI (B). (C) WT-PKCδ- and PKCδ-Y313F-overexpressing cultures were treated for 5 min with vehicle or 5 mM H_2O_2. Cell lysates were subjected to immunoblot analysis for PKCδ protein and Tyr^{313}/Ser^{359} phosphorylation. (D) WT-PKCδ- or PKCδ-S359A-overexpressing cultures were treated for 20 min with vehicle or 200 nM PMA. Cell lysates were subjected to immunoblot analysis with the anti-PKC substrate and anti-TXR motif PSSAs as well as with antibodies that recognize activated/phosphorylated forms of PKD. A purified myofibrillar fraction also was subjected to immunoblot analysis with the anti-PKC substrate and anti-TXR motif PSSAs. All results were replicated in two to four separate experiments.

using two different experimental approaches (multiple-reaction monitoring–mass spectrometry and Western blotting with a PSSA) show that PKCδ-ΔC2 is recovered from cells without Ser^{359} phosphorylation, indicating that Ser^{359} phosphorylation is disrupted by the C2 domain deletion. Mutagenesis studies implicate this Ser^{359} phosphorylation defect as the mechanism underlying PKCδ-ΔC2's altered catalytic activity. These results suggest that the C2 domain in the inactive enzyme is positioned to protect Ser^{359} from cellular phosphatases and that a C2 domain deletion or a mechanism that displaces the C2 domain from this site (such as the docking interaction with the Tyr^{313}-phosphorylated hinge region) decreases Ser^{359} phosphorylation. This model is supported by cell-based studies showing that the H_2O_2-dependent increase in Tyr^{313} phosphorylation is associated with a decrease in Ser^{359} phosphorylation on WT-PKCδ but not the PKCδ-Y313F mutant.

The G-loop sequence is highly conserved in many protein kinases. Structural studies of PKA and several PKCs show that the G loop forms a flexible clamp that orients the γ-phosphate of ATP for transfer to substrate; localized changes in the position of this loop influence the kinetics of nucleotide binding and the phosphoryl transfer reaction. The Ser in the GKGSFG sequence in PKA is strategically positioned at the tip of the G loop at the entrance to the ATP-binding cleft, in close proximity to the P site on substrates (Fig. 7A). This site in the G loop of several other kinases has been implicated in the control of catalytic activity. For example, CDK1 (a regulator of the eukaryotic cell cycle) is maintained in an inactive conformation by inhibitory phosphorylations at Y^{15} and,

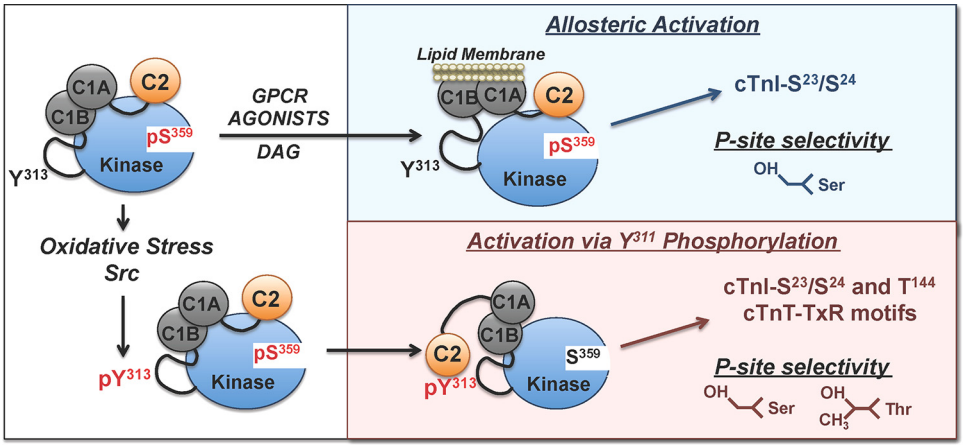

FIG 9 Schematic of the agonist-specific activation mechanisms for PKCδ. See the text. GPCR, G protein-coupled receptor.

to a lesser extent, in the adjacent T^{14} in its ATP-binding GEGTYG motif; dephosphorylation of these sites at the onset of mitosis leads to enzyme activation (23). The nononcogenic c-ABL proto-oncogene is activated by a G-loop GGGQ(Y253F)G substitution (24); point mutations in Bcr-Abl (the constitutively active tyrosine kinase that drives malignant transformation in chronic myeloid leukemia) that alter G-loop Y^{253} phosphorylation confer drug resistance and enhanced oncogenicity (25, 26). Finally, there is evidence that c-Raf is maintained in a basal autoinhibited state through G-loop autophosphorylation and that c-Raf becomes activated (leading to a paradoxical activation of the mitogen-activated protein kinase pathway) by ATP-competitive Raf inhibitors that prevent G-loop autoinhibitory phosphorylation (27). However, posttranslational modifications at the G loop that regulate PKC (or PKA) activities have never been reported. This study identifies G-loop regulation of two key aspects of PKCδ's enzymology, as follows.

(i) Phosphomimetic or bulky substitutions at Ser^{359} inhibit PKCδ phosphorylation of TXR motifs on cTnI and cTnT but not cTnI phosphorylation at Ser^{23}/Ser^{24}. Ser^{359} phosphorylation could in theory influence PKCδ's substrate specificity indirectly by restructuring the catalytic pocket to accommodate a wider range of phosphorylation motifs or by modulating docking interactions that control substrate alignment in the catalytic pocket. However, experiments with short peptide substrates harboring single-residue P-site substitutions show that a phosphomimetic substitution at position 359 prevents phosphorylation of Thr-phosphoacceptor sites (presumably due to steric clash with the Thr methyl group); Ser-phosphoacceptor sites are not affected. Hence, while recent literature has focused on consensus phosphorylation motifs (residues that are either preferred or deselected at positions flanking the P site on a particular substrate) as the key determinant of enzyme substrate specificity, our studies show that PKCδ activity can also vary depending upon whether the P site is a Ser or Thr residue. The novelty of this observation deserves emphasis. While Chen et al. recently identified the "DFG +1" residue (a residue immediately downstream of a conserved Asp-Phe-Gly sequence) in the activation segment as a structural determinant that defines the inherent P-site specificity of various Ser/Thr kinases (28), a dynamically regulated posttranslational modification that can alter P-site specificity in a stimulus-specific manner is unprecedented. This study implicates ATP-positioning loop phosphorylation at Ser^{359} as a mechanism that dynamically regulates the P-site specificity of PKCδ.

(ii) An S359A substitution imparts a high level of lipid-independent catalytic activity. The PKCδ-S359A mutant is a constitutively active enzyme; it acts (much like the lipid-independent form of PKCδ that accumulates in cells subjected to oxidative stress) to phosphorylate substrates throughout the cell, not just on lipid membranes. This suggests that the ATP-positioning loop site participates in an autoinhibitory intramolecular interaction and that this intramolecular interaction is dynamically controlled by G-loop phosphorylation. This result is consistent with recent structural evidence that the basal catalytic activity of PKCβII is limited by an autoinhibitory interaction between the ATP binding site and the C1 domain (29).

Several aspects of our study have implications for the pathogenesis and/or treatment of clinical disease. First, the observation that phosphomimetic and bulky hydrophobic amino acid substitutions at Ser^{359} produce similar changes in PKCδ activity indicates that regulation is due to steric hindrance from the bulky phosphate group, rather than from the negative charge, at this site. This suggests that other bulky substitutions might have similar consequences. This may be pertinent to the diabetic state, where both PKC and increased protein O-GlcNAcylation contribute to cardiac dysfunction (30). Studies to date suggest that hyperglycemia activates PKC by inducing oxidative stress or increasing *de novo* DAG synthesis. However, the evidence that Ser^{349} in PKCα's G loop is a target for O-GlcNAcylation (addition of a bulky sugar moiety [21]) suggests that PTMs directed at the G loop might also underlie hyperglycemia-induced changes in PKC isoform activity.

Second, while PKCδ-ΔC2 was used in this study as a molecular tool to interrogate the structural determinants that regulate PKCδ catalytic activity, this construct resembles a truncated PKCδ isoform that is expressed in a developmentally regulated manner as a result of alternative splicing in mouse testis (31). Since disease-specific changes in PKCδ mRNA splicing have recently been identified in certain heart failure phenotypes (32, 33), a truncated PKCδ isoform might be a component of the altered cardiac transcriptome that contributes to pathological cardiac stress responses.

Finally, this study identifies a protein-protein interaction involving the C2 domain and the Tyr^{313}-phosphorylated hinge region that calibrates PKCδ's substrate specificity by controlling phosphorylation at Ser^{359}. This mechanism is prominent during oxidative stress, where Src activation leads to an increase in PKCδ-Tyr^{313} phosphorylation; PKCδ-Tyr^{313} phosphorylation is not a feature of G protein-coupled receptor-activated signaling responses. Stimulus-specific differences in PKCδ phosphorylation at Tyr^{313} and Ser^{359} that impact substrate specificity provide a very plausible explanation for PKCδ's diverse roles in both the pathogenesis of ischemia-reperfusion injury and as a mediator of ischemic preconditioning (a cardioprotective mechanism that mitigates ischemic injury) (34). Stimulus-specific signaling modes for PKCδ that link to functionally distinct cellular responses could also explain why recent efforts to bring a PKCδ inhibitor compound to the clinic for the treatment of ischemic cardiac injury met with failure; the trial involved a PKCδ inhibitor that was not designed to discriminate between pools of PKCδ with distinct phosphorylation patterns at Tyr^{313} and Ser^{359}. Our results suggest that an inhibitor compound designed to prevent the C2 domain-pTyr^{313} interaction (and/or Ser^{359} dephosphorylation) might selectively block the redox-activated PKCδ-dependent signaling responses that contribute to ischemic injury and offer significant therapeutic advantage.

ACKNOWLEDGMENTS

This work was supported by HL77860 (S.F.S) and grants to the Johns Hopkins Innovation Proteomics Center in Heart Failure (HHSN268201000032C and NHLBI-HV-10-05 to J.E.V.E.). S.F.S. was supported by an award from the NIH (1DP2 CA186752-01) and by an AHA Scientist Development Grant (13SDG14270009).

REFERENCES

1. **Stahelin RV, Digman MA, Medkova M, Ananthanarayanan B, Rafter JD, Melowic HR, Cho W.** 2004. Mechanism of diacylglycerol-induced membrane targeting and activation of protein kinase Cδ. J Biol Chem **279:**29501–29512. http://dx.doi.org/10.1074/jbc.M403191200.
2. **Dekker LV, Parker PJ.** 1997. Regulated binding of the protein kinase C substrate GAP-43 to the V0/C2 region of protein kinase C-δ. J Biol Chem **272:**12747–12753. http://dx.doi.org/10.1074/jbc.272.19.12747.
3. **Lopez-Lluch G, Bird MM, Canas B, Godovac-Zimmerman J, Ridley A, Segal AW, Dekker LV.** 2001. Protein kinase Cδ C2-like domain is a binding site for actin and enables actin redistribution in neutrophils. Biochem J **357:**39–47. http://dx.doi.org/10.1042/0264-6021:3570039.
4. **Benes CH, Wu N, Elia AE, Dharia T, Cantley LC, Soltoff SP.** 2005. The C2 domain of PKCδ is a phosphotyrosine binding domain. Cell **121:**271–280. http://dx.doi.org/10.1016/j.cell.2005.02.019.
5. **Konishi H, Yamauchi E, Taniguchi H, Yamamoto T, Matsuzaki H, Takemura Y, Ohmae K, Kikkawa U, Nishizuka Y.** 2001. Phosphorylation sites of protein kinase Cδ in H_2O_2-treated cells and its activation by tyrosine kinase in vitro. Proc Natl Acad Sci U S A **98:**6587–6592. http://dx.doi.org/10.1073/pnas.111158798.
6. **Steinberg SF.** 2008. Structural basis of protein kinase C isoform function. Physiol Rev **88:**1341–1378. http://dx.doi.org/10.1152/physrev.00034.2007.
7. **Rybin VO, Guo J, Sabri A, Elouardighi H, Schaefer E, Steinberg SF.** 2004. Stimulus-specific differences in protein kinase C-δ localization and activation mechanisms in cardiomyocytes. J Biol Chem **279:**19350–19361. http://dx.doi.org/10.1074/jbc.M311096200.
8. **Rybin VO, Guo J, Gertsberg Z, Feinmark SJ, Steinberg SF.** 2008. Phorbol 12-myristate 13-acetate-dependent protein kinase C-δ-Tyr^{313} phosphorylation in cardiomyocyte caveolae. J Biol Chem **283:**17777–17788. http://dx.doi.org/10.1074/jbc.M800333200.
9. **Sumandea MP, Rybin VO, Hinken AC, Wang C, Kobayashi T, Harleton E, Sievert G, Balke CW, Feinmark SJ, Solaro RJ, Steinberg SF.** 2008. Tyrosine phosphorylation modifies PKCδ-dependent phosphorylation of cardiac troponin I. J Biol Chem **283:**22680–22689. http://dx.doi.org/10.1074/jbc.M802396200.
10. **Lu W, Finnis S, Xiang C, Lee HK, Markowitz Y, Okhrimenko H, Brodie C.** 2007. Tyrosine^{313} is phosphorylated by c-Abl and promotes the apoptotic effect of PKCδ in glioma cells. Biochem Biophys Res Commun **352:**431–436. http://dx.doi.org/10.1016/j.bbrc.2006.11.028.
11. **Nakashima H, Frank GD, Shirai H, Hinoki A, Higuchi S, Ohtsu H, Eguchi K, Sanjay A, Reyland ME, Dempsey PJ, Inagami T, Eguchi S.** 2008. Novel role of protein kinase C-δ Tyr^{313} phosphorylation in vascular smooth muscle cell hypertrophy by angiotensin II. Hypertension **51:**232–238. http://dx.doi.org/10.1161/HYPERTENSIONAHA.107.101253.
12. **Rybin VO, Sabri A, Short J, Braz JC, Molkentin JD, Steinberg SF.** 2003. Cross-regulation of novel protein kinase C (PKC) isoform function in cardiomyocytes. Role of PKC-epsilon in activation loop phosphorylations and PKC-delta in hydrophobic motif phosphorylations. J Biol Chem **278:**14555–14564. http://dx.doi.org/10.1074/jbc.M212644200.
13. **Aprigliano O, Rybin VO, Pak E, Robinson RB, Steinberg SF.** 1997. β_1- And β_2-adrenergic receptors exhibit differing susceptibility to muscarinic accentuated antagonism. Am J Physiol **272:**H2726–H2735.
14. **Rybin VO, Xu X, Lisanti MP, Steinberg SF.** 2000. Differential targeting of β-adrenergic receptor subtypes and adenylyl cyclase to cardiomyocyte caveolae: A mechanism to functionally regulate the cAMP signaling pathway. J Biol Chem **275:**41447–41457. http://dx.doi.org/10.1074/jbc.M006951200.
15. **Zhang P, Kirk JA, Ji W, dos Remedios CG, Kass DA, Van Eyk JE, Murphy AM.** 2012. Multiple reaction monitoring to identify site-specific troponin I phosphorylated residues in the failing human heart. Circulation **126:**1828–1837. http://dx.doi.org/10.1161/CIRCULATIONAHA.112.096388.
16. **Sivaramakrishnan S, Spudich JA.** 2011. Systematic control of protein interaction using a modular ER/K alpha-helix linker. Proc Natl Acad Sci U S A **108:**20467–20472. http://dx.doi.org/10.1073/pnas.1116066108.
17. **Ritt M, Guan JL, Sivaramakrishnan S.** 2013. Visualizing and manipulating focal adhesion kinase regulation in live cells. J Biol Chem **288:**8875–8886. http://dx.doi.org/10.1074/jbc.M112.421164.
18. **Sivaramakrishnan S, Spink BJ, Sim AY, Doniach S, Spudich JA.** 2008. Dynamic charge interactions create surprising rigidity in the ER/K alpha-helical protein motif. Proc Natl Acad Sci U S A **105:**13356–13361. http://dx.doi.org/10.1073/pnas.0806256105.
19. **Rybin VO, Guo J, Harleton E, Feinmark SJ, Steinberg SF.** 2009. Regulatory autophosphorylation sites on protein kinase C-delta at Thr^{141} and Thr^{295}. Biochemistry **48:**4642–4651. http://dx.doi.org/10.1021/bi802171c.
20. **Seidler J, Adal M, Kubler D, Bossemeyer D, Lehmann WD.** 2009. Analysis of autophosphorylation sites in the recombinant catalytic subunit alpha of cAMP-dependent kinase by nano-UPLC-ESI-MS/MS. Anal Bioanal Chem **395:**1713–1720. http://dx.doi.org/10.1007/s00216-009-2932-4.
21. **Robles-Flores M, Melendez L, Garcia W, Mendoza-Hernandez G, Lam TT, Castaneda-Patlan C, Gonzalez-Aguilar H.** 2008. Posttranslational modifications on protein kinase C isozymes. Effects of epinephrine and phorbol esters. Biochim Biophys Acta **1783:**695–712. http://dx.doi.org/10.1016/j.bbamcr.2007.07.011.
22. **Ozgen N, Obreztchikova M, Guo J, Elouardighi H, Dorn GW, Wilson BA, Steinberg SF.** 2008. Protein kinase D links Gq-coupled receptors to cAMP response element-binding protein (CREB)-Ser^{133} phosphorylation in the heart. J Biol Chem **283:**17009–17019. http://dx.doi.org/10.1074/jbc.M709851200.
23. **Norbury C, Blow J, Nurse P.** 1991. Regulatory phosphorylation of the p34cdc2 protein kinase in vertebrates. EMBO J **10:**3321–3329.
24. **Allen PB, Wiedemann LM.** 1996. An activating mutation in the ATP binding site of the ABL kinase domain. J Biol Chem **271:**19585–19591. http://dx.doi.org/10.1074/jbc.271.32.19585.
25. **Skaggs BJ, Gorre ME, Ryvkin A, Burgess MR, Xie Y, Han Y, Komisopoulou E, Brown LM, Loo JA, Landaw EM, Sawyers CL, Graeber TG.** 2006. Phosphorylation of the ATP-binding loop directs oncogenicity of drug-resistant BCR-ABL mutants. Proc Natl Acad Sci U S A **103:**19466–19471. http://dx.doi.org/10.1073/pnas.0609239103.
26. **Griswold IJ, MacPartlin M, Bumm T, Goss VL, O'Hare T, Lee KA, Corbin AS, Stoffregen EP, Smith C, Johnson K, Moseson EM, Wood LJ, Polakiewicz RD, Druker BJ, Deininger MW.** 2006. Kinase domain mutants of Bcr-Abl exhibit altered transformation potency, kinase activity, and substrate utilization, irrespective of sensitivity to imatinib. Mol Cell Biol **26:**6082–6093. http://dx.doi.org/10.1128/MCB.02202-05.
27. **Holderfield M, Merritt H, Chan J, Wallroth M, Tandeske L, Zhai H, Tellew J, Hardy S, Hekmat-Nejad M, Stuart DD, McCormick F, Nagel TE.** 2013. RAF inhibitors activate the MAPK pathway by relieving inhib-

itory autophosphorylation. Cancer Cell **23:**594–602. http://dx.doi.org/10.1016/j.ccr.2013.03.033.
28. **Chen C, Ha BH, Thevenin AF, Lou HJ, Zhang R, Yip KY, Peterson JR, Gerstein M, Kim PM, Filippakopoulos P, Knapp S, Boggon TJ, Turk BE.** 2014. Identification of a major determinant for serine-threonine kinase phosphoacceptor specificity. Mol Cell **53:**140–147. http://dx.doi.org/10.1016/j.molcel.2013.11.013.
29. **Leonard TA, Rozycki B, Saidi LF, Hummer G, Hurley JH.** 2011. Crystal structure and allosteric activation of protein kinase C-βII. Cell **144:**55–66. http://dx.doi.org/10.1016/j.cell.2010.12.013.
30. **McLarty JL, Marsh SA, Chatham JC.** 2013. Post-translational protein modification by O-linked *N*-acetyl-glucosamine: Its role in mediating the adverse effects of diabetes on the heart. Life Sci **92:**621–627. http://dx.doi.org/10.1016/j.lfs.2012.08.006.
31. **Kawaguchi T, Niino Y, Ohtaki H, Kikuyama S, Shioda S.** 2006. New PKCδ family members, PKCδIV, δV, δVI, and δVII are specifically expressed in mouse testis. FEBS Lett **580:**2458–2464. http://dx.doi.org/10.1016/j.febslet.2006.03.084.
32. **Song HK, Hong SE, Kim T, Kim do, H.** 2012. Deep RNA sequencing reveals novel cardiac transcriptomic signatures for physiological and pathological hypertrophy. PLoS One **7:**e35552. http://dx.doi.org/10.1371/journal.pone.0035552.
33. **Ricci M, Xu Y, Hammond HL, Willoughby DA, Nathanson L, Rodriguez MM, Vatta M, Lipshultz SE, Lincoln J.** 2012. Myocardial alternative RNA splicing and gene expression profiling in early stage hypoplastic left heart syndrome. PLoS One **7:**e29784. http://dx.doi.org/10.1371/journal.pone.0029784.
34. **Steinberg SF.** 2012. Cardiac actions of protein kinase C isoforms. Physiology (Bethesda) **27:**130–139. http://dx.doi.org/10.1152/physiol.00009.2012.